Pseudo-Symmetries of Anosov Maps and Spectral Statistics

J.P. Keating, F. Mezzadri
Basic Research Institute in the Mathematical Sciences
HP Laboratories Bristol
HPL-BRIMS-1999-09
26th October, 1999*

Anosov maps, quantum chaos, spectral statistics, arithmetical symmetries

The statistics of the quantum eigenvalues of certain families of nonlinear maps on the two-torus are found not to belong to the universality classes one would expect from the symmetries of the (classical) dynamics the maps generate. These anomalies are shown to be caused by arithmetical quantum symmetries which do not have a classical limit. They are related to the dynamics generated by associated linear torus maps on particular rational lattices that form the support of the quantum Wigner functions.

0   Introduction

It has been suggested that, in the semiclassical limit, the spectral statistics of classically chaotic systems are generically determined solely by the symmetries of their quantum dynamics, and that, in that limit, they coincide with those of random matrix theory (RMT) [12, 6]. This idea is central to our understanding of the quantum properites of nonintegrable systems, and is supported by extensive numerical evidence [6] and semiclassical theory [24, 5, 11]. Its application obviously requires a knowledge of the relevant quantum symmetries. Usually these can be found by quantizing the corresponding classical symmetries. Our purpose here is to describe a family of examples for which this procedure fails. Specifically, we construct a class of quantum symmetries for certain nonlinear automorphisms of the two-torus which determine the spectral statistics but have no classical limit.

The systems we concentrate on correspond to linear hyperbolic automorphisms of the two-torus, sometimes known as *cat maps*, perturbed by nonlinear shears, the perturbations being small enough for the resulting maps to remain hyperbolic [1, 2]. We shall refer to the perturbed maps as *Anosov maps*. The quantization of the cat maps themselves was developed by Hannay and Berry [23], and since then their quantum [15, 17, 19, 20, 21, 29, 30, 34] and semiclassical [14, 16, 25, 26, 32, 33] properties have been much studied, mainly to investigate the influence of classical chaos on quantum eigenvalues and eigenfunctions. Shear-perturbed cat maps were first quantized by Basilio de Matos and Ozorio de Almeida [4], and have also been much studied [9, 28], especially in connection with the link to random matrix theory [4, 7, 18].

The eigenvalues of a generic quantum map whose classical limit is chaotic and which possesses at least one antiunitary symmetry are, in the semiclassical limit, expected to be correlated like those of random unitary and symmetric matrices. These matrices constitute the Circular Orthogonal Ensemble (COE) of random matrix theory. Likewise, the spectral statistics of a classically chaotic quantum map which does not have any antiunitary symmetries are expected to be those of random unitary matrices, which form the Circular Unitary Ensemble (CUE). Finally, the spectra of maps which possess unitary symmetries are expected to behave like an independent superposition of the corresponding number of random-matrix-correlated subspectra. The cat maps are known to be non-generic with respect to their spectral statistics [23, 26], whilst numerical investigations suggest that nonlinearly perturbed maps do behave generically.

For the cat maps, unitary symmetries can be constructed by quantizing canonical symmetry transformations (e.g. parity) of the classical dynamics using the Hannay-Berry formalism. Likewise, antiunitary quantum symmetries can be constructed from anticanonical classical symmetries (e.g. time reversal). However, we will show that there are other quantum symmetries, both unitary and antiunitary, which cannot be found in this way. These *pseudo-symmetries* are directly related to the arithmetical nature of the cat maps, and are responsible for their non-generic spectral statistics. When the cat maps are nonlinearly perturbed, their arithmatic character is destroyed, and so it might be imagined that only those symmetries with a classical limit remain. We will demonstrate that this is not necessarily the case: under certain general classes of perturbations (in particular, those used in previous studies of perturbed cat maps) some pseudo-symmetries also survive, and these have an important effect on the quantum

spectral statistics.

Our construction of the pseudo-symmetries is based on the time evolution of the quantum Wigner functions. For torus maps, all Wigner functions have support on a $2N \times 2N$ lattice, where N, the dimension of the Hilbert space, plays the role of the inverse of Planck's constant. In the case of the cat maps, the time evolution of any Wigner function is given by the action of the underlying classical map on this quantum lattice. The pseudo-symmetries, both unitary and antiunitary, then correspond to classical symmetries of the quantum-lattice dynamics. They have no classical limit, in that they are not symmetries of the dynamics off the Wigner lattice. Nevertheless, they give rise to degeneracies amongst the periodic orbit contributions to the semiclassical trace formula.

These pseudo-symmetries have also been studied for the cat maps by Kurlberg and Rudnick [30], mainly in the context of their influence on the quantum eigenfunctions and their similarity to the Hecke operators associated with the laplacian on arithmetic surfaces of constant negative curvature, which are responsible for the non-generic properties of those systems [13]. Our main results, which formed the basis of [31], relate to spectral statistics, and in particular to nonlinearly perturbed cat maps. They have previously been summerized and discussed informally in [27].

The outline of this paper is as follows. In order to motivate the subsequent analysis, we start in Section 1 with a brief review of the (non-generic) spectral statistics of the cat maps and then demonstrate that there are Anosov maps whose quantum statistics are also anomalous from the point of view of their classical symmetries and/or the boundary conditions used in their quantization. We construct the pseudo-symmetries described above in Section 2. Finally, some implications of this work are discussed in Section 3. A number of the calculations are described in appendices.

1   Some torus maps, their symmetries, and spectral statistics

Our purpose in this section is to illustrate the fact that the symmetries of a torus map do not necessarily determine its quantum spectral statistics. This is well-known in the case of the cat maps, whose symmetries were classified in [3]. We show that it also true for nonlinear perturbations of the cat maps, by focussing on several anomalies in their eigenvalue correlations. For instance, we give examples of quantum maps with the same classical symmetries but different spectral statistics. This suggests the existence of quantum symmetries with no classical counterpart (and so a failure of what one might be termed strict correspondence in this respect), which we construct in Section 2.

The cat maps - the linear hyperbolic automorphisms of the two-torus - are a family of completely chaotic dynamical systems. A given cat map A may be represented by the action of a 2×2 matrix modulo 1 (for dynamics on the unit two-torus). Thus

$$\begin{pmatrix} q' \\ p' \end{pmatrix} = A \begin{pmatrix} q \\ p \end{pmatrix} \bmod 1, \tag{1.1}$$

where the torus coordinates q and p are taken to represent a position variable and its conjugate momentum respectively. The elements of this matrix must be integers in order for the mapping to be continuous on the torus; the matrix must have unit determinant

for the map to be canonical, *i.e.* orientation and area preserving; and the modulus of the trace of the matrix must be greater than two, in order to guarantee that all orbits are hyperbolically unstable [2].

The quantum map associated with A is an $N \times N$ unitary matrix U, where N plays the role of the inverse of Planck's constant. Hannay and Berry [23] gave a method for computing U in terms of the elements of A.

Even though the cat maps are paradigms of hyperbolic dynamics, the spectral statistics of U are non-generic from the point of view of the random-matrix conjecture described in the introduction: the spectrum is characterised by semiclassically large degeneracies [25, 26, 30] and does not show the eigenvalue repulsion which is typical of chaotic systems. We illustrate this with a specific example below.

First, however, we recall the general definitions of canonical and anticanonical symmetries as applied to maps, and of quantum unitary and antiunitary symmetries. Let ϕ and γ be two canonical maps (not necessarily linear); γ is a canonical symmetry of ϕ if

$$\gamma \circ \phi \circ \gamma^{-1} = \phi. \tag{1.2}$$

Likewise, the transformation β is said to be an anticanonical symmetry of ϕ if

$$\beta \circ \phi \circ \beta^{-1} = \phi^{-1}, \tag{1.3}$$

$\beta^2 = I$ and $\det D\beta = -1$, where $D\beta$ is the differential of β.

Analogously for quantum maps, if U and W are two unitary matrices, then W is said to be a unitary symmetry of U if they commute; and if K is an antiunitary operator, *i.e.* if

$$\langle K\psi | K\phi \rangle = \langle \phi | \psi \rangle \tag{1.4}$$

for all $|\phi\rangle$ and $|\psi\rangle$, then K is said to be an antiunitary symmetry of U if

$$KUK^{-1} = U^{-1}. \tag{1.5}$$

Unitary (antiunitary) symmetries in quantum mechanics generally correspond to canonical (anticanonical) symmetries in classical mechanics. One example of an antiunitary and anticanonical symmetry is time-reversal. Quantum mechanically, time-reversal is generated by the complex conjugation operator in the position representation. Its classical limit for torus maps is

$$T = \begin{pmatrix} 1 & 0 \\ 0 & -1 \end{pmatrix}, \tag{1.6}$$

which clearly reverses the sign of momentum while leaving position unchanged.

Let us now return to the spectral statistics of the quantum cat maps. In Figure 1 we show the cumulative spacing distribution and number variance of the quantum map corresponding to

$$A = \begin{pmatrix} 10 & 3 \\ 33 & 10 \end{pmatrix}. \tag{1.7}$$

[Figure 1 about here.]

Here the cumulative spacing distribution $Ip(s)$ is defined as the probability that the distance between two consecutive eigenangles is less than s, in units where the mean spacing is one, *i.e.*

$$Ip(s) = \int_0^s p(s)ds, \tag{1.8}$$

where $p(s)$ is the spacing distribution. The number varaince $V(L)$ is likewise defined in the following way. Let $n(x, L)$ denote the number of eigenangles in an interval of length L centred at x. The average of n with respect to x is obviously L (again in units where the mean spacing is one); $V(L)$ is then the variance of $n(x, L)$:

$$V(L) = \frac{1}{N} \int_0^N \left(n(x, L) - L \right)^2 dx. \tag{1.9}$$

For the eigenvalues of random matrices, $V(L)$ grows as $\eta \log L$, where $\eta = 1/\pi^2$ if the system possesses no antiunitary symmetry (CUE) and $\eta = 2/\pi^2$ if such a symmetry is present (COE). Based on the random-matrix conjecture, one would thus expect these results to describe the spectral statistics of generic, classically chaotic systems in the semiclassical limit, that is, as $N \to \infty$ for maps. For large but finite N, semiclassical asymptotics [5] predicts that the random-matrix form should hold for $1 << L << L_{max}(N)$, where $L_{max}(N) \to \infty$ as $N \to \infty$, and that when $L >> L_{max}$ the number variance saturates into a series of non-universal, (*i.e.* system dependent), quasi-periodic oscillations, which are related to the short classical periodic orbits.

The only symmetries of the map (1.7) are parity and time reversal. Clearly the eigenangle distributions are completely different from the RMT predictions. This has previously been understood in terms of the number-theoretical properties of both the classical periodic orbits and the quantum eigenvalues of the cat maps [25, 26]. In Section 2.1 we give an alternative interpretation.

In order to destroy the (presumably) non-generic features of the quantum cat maps, Basilio de Matos and Ozorio de Almeida [4] quantized nonlinear automorphisms of the two-torus. According to a theorem of Anosov [1], the cat maps are *structurally stable*, which means that every diffeomorphism ϕ sufficiently close to a given cat map A is conjugate to A by means of some homeomorphism H, *i.e.* $\phi = H \circ A \circ H^{-1}$. This theorem has important consequences. If A is slightly perturbed, the new map is topologically the same as A and preserves all the chaotic properties of the unperturbed map, in particular the instability of the orbits: the classical mechanics are qualitatively the same. Therefore, by introducing a small nonlinear perturbation, the orbits are slightly deformed and are still hyperbolic; but at the same time the number theoretical characterisation of the system is lost.

The particular perturbations considered in [4] were nonlinear shears in momentum:

$$P_p(q, p) = (q, p + k_p F(q)), \tag{1.10}$$

where $F(q)$ is periodic and, in order to break parity, must not be an odd function of q. Such perturbations can be quantized easily; the corresponding quantum map is diagonal

in the position representation [4]. In Figure 2 the spectral statistics of the map (1.7) perturbed with the shear (1.10) are plotted. The function $F(q)$ used was

$$F(q) = \frac{1}{2\pi}(\cos 2\pi q - \cos 4\pi q). \tag{1.11}$$

[Figure 2 about here.]

The map (1.7) is invariant under parity and time-reversal, the shear (1.10) is invariant under time-reversal only, and so the only symmetry of ϕ is the anticanonical symmetry generated by $T \circ P_p(q, p)$. One thus expects the spectral statistics to be those of the COE, as observed. This confirms the results (for a different A) reported in [4].

1.1 Maps with no anticanonical symmetries

We now perturb a cat map possessing no anticanonical symmetries with the shear (1.10). The corresponding Anosov map ϕ will thus have no symmetries, and so one might expect the spectral statistics to be CUE.

The map we use is

$$A = \begin{pmatrix} 4 & 9 \\ 7 & 16 \end{pmatrix} \tag{1.12}$$

which, as shown in [3] does not have any symmetries except parity. Indeed, it has the minimum trace for which it is possible to find a cat map with no anticanonical symmetry.

In Figure 3 we show the spectral statistics of the quantum map corresponding to the map (1.12) perturbed with the shear (1.10). Surprisingly the statistics are COE, rather than CUE, even though the classical dynamics does not possess any anticanonical symmetries.

[Figure 3 about here.]

We now perturb the map (1.12) with a composition of two shears: the perturbation (1.10) and a similar shear in position

$$P_q(q, p) = (q + k_q G(p), p), \tag{1.13}$$

where $G(p)$ is taken to be periodic and odd, so that time-reversal is a symmetry of $P_q(q, p)$. (The shear in momentum is always invariant under time-reversal). Specifically we use

$$G(p) = \frac{1}{2\pi}(\sin 4\pi p - \sin 2\pi p). \tag{1.14}$$

The composition

$$P_r(q, p) = P_p \circ P_q(q, p) \tag{1.15}$$

is invariant under time-reversal up to terms that are second order in the perturbation parameters. For k_p and k_q of the order of 10^{-2} (approximately the upper limit allowed

6

by Anosov's theorem) $k_p k_q \sim 10^{-4}$. In this parameter range we can thus consider time-reversal to be a symmetry of (1.15). Parity does not commute with $P_r(q, p)$ because $F(q)$ is not odd. This means that effectively the map

$$\phi' = A \circ P_p \circ P_q(q, p) \tag{1.16}$$

does not have any symmetries, like $\phi = A \circ P_p(q, p)$.

In Figure 4 the statistics of the quantum map corresponding to ϕ' are plotted. This time they are CUE, as expected, even though the map ϕ' has exactly the same classical symmetry properties as ϕ.

[Figure 4 about here.]

In Section 2.2 we shall see that the cause of this anomalous behaviour in the spectral statistics is the existence of a class of quantum symmetries of the cat maps which do not have a classical limit. Moreover, we will show that any cat map with no anticanonical symmetries perturbed in the same way as (1.12) would exhibit the same behaviour. The map (1.12) is thus a typical, rather than an isolated example.

1.2 Anosov maps and boundary conditions

The topology of the two-torus is that of the unit square whose opposite sides are identified. Therefore, any wavefunction describing the quantum state of a torus map must be periodic up to a phase factor in both the position and momentum representations:

$$\langle q + m_1 | \psi \rangle = \psi(q + j) = e^{2\pi i j \theta_2} \psi(q), \tag{1.17a}$$

$$\langle p + m_2 | \psi \rangle = \tilde{\psi}(p + k) = e^{-2\pi i k \theta_1} \tilde{\psi}(p), \tag{1.17b}$$

for any integers j and k. In order for superpositions of states to be quasiperiodic, the phases $\boldsymbol{\theta} = (\theta_1, \theta_2)$ must be the same for all states representing the system. We denote the Hilbert space of quasiperiodic vectors by $\mathcal{H}(\boldsymbol{\theta})$. The phases $\boldsymbol{\theta} = (\theta_1, \theta_2)$ can be thought of as *boundary conditions*. The quantum maps used in the computations described above were obtained by quantization with periodic boundary conditions.

We note in passing that the behaviour of a quantum state under lattice translations is analogous to the phase factor which a wavefunction describing a charged particle in an electromagnetic field acquires under a gauge transformation of the potential.

Anosov maps can be quantized only for a finite number of rational values of the phases $\boldsymbol{\theta} = (\theta_1, \theta_2)$ [28], namely those which satisfy

$$A \cdot \boldsymbol{\theta} = \boldsymbol{\theta} + \frac{N}{2} \mathbf{v} \bmod 1, \tag{1.18}$$

where A is the unperturbed map and $\mathbf{v}$ is an integer vector which depends on A. If $AA^T = I \bmod 2$ the above equation reduces to

$$A \cdot \boldsymbol{\theta} = \boldsymbol{\theta} \bmod 1. \tag{1.19}$$

Without loss of generality, we shall henceforth only consider maps such that $AA^T = I \bmod 2$; the matrices (1.7) and (1.12) are of this type.

The boundary conditions $\boldsymbol{\theta}$ affect the spectral statistics of Anosov maps nontrivially. Using semiclassical techniques, we now show that an appropriate choice of the parameters $\boldsymbol{\theta}$ may induce a COE $\rightarrow$ CUE transition when the classical mechanics is time-reversal invariant. A quantum mechanical argument for this will be given later.

First, we need a semiclassical approximation for the density of states, *i.e.* a trace formula for Anosov maps. The density of states for a general map is defined by

$$d(\alpha) = \sum_{j=1}^{N} \sum_{k=-\infty}^{\infty} \delta(\alpha - \alpha_j - 2\pi k), \tag{1.20}$$

where the j-sum includes all of the eigenvalues α_j of the quantum map. Using the Poisson summation formula

$$\sum_{j=-\infty}^{\infty} \delta(x - j) = \sum_{k=-\infty}^{\infty} \exp(2\pi i x k), \tag{1.21}$$

this may be written

$$d(\alpha) = \frac{N}{2\pi} + \frac{1}{\pi} \operatorname{Re} \sum_{k=1}^{\infty} \operatorname{Tr}\left(U^k\right) e^{-ik\alpha}. \tag{1.22}$$

In the semiclassical limit, $\operatorname{Tr}(U^k)$ can, for any Anosov map sufficiently close to a cat map, be expressed as a sum over the fixed points of $\boldsymbol{\phi}^k$:

$$\operatorname{Tr}\left(U_{\boldsymbol{\phi}}^k\right) \simeq \sum_{\mathbf{m} \in \square} \frac{1}{\sqrt{-R_{\mathbf{m}}^{(k)}}} \exp\left[2\pi i N S_{\boldsymbol{\phi}^k}\left(\mathbf{m}, \boldsymbol{\theta}\right)\right]. \tag{1.23}$$

Here $\mathbf{m} = (m_1, m_2)$ is an integer vector, defined by

$$\boldsymbol{\phi}^k(\mathbf{z}_{\mathrm{f}}) - \mathbf{z}_{\mathrm{f}} = \mathbf{m}, \tag{1.24}$$

whose components are the winding numbers associated with the fixed point $\mathbf{z}_{\mathrm{f}} = (q_f, p_f)$. Winding numbers and fixed points are therefore in one-to-one correspondence and we shall indicate a fixed point with either $\mathbf{z}_{\mathrm{f}}$ or $\mathbf{m}$. The symbol $\square$ denotes the curvilinear parallelogram which is the image of the unit square under the action of $\boldsymbol{\phi}^k - \mathbf{I}$. The argument of the exponential in (1.23) is the *effective action*:

$$S_{\boldsymbol{\phi}^k}(\mathbf{m}, \boldsymbol{\theta}) = \boldsymbol{\theta} \wedge \mathbf{m}/N + S_{\boldsymbol{\phi}^k}(q_{\mathrm{f}}(\mathbf{m}) + m_1, q_{\mathrm{f}}(\mathbf{m})) - m_2 q_{\mathrm{f}}(\mathbf{m}), \tag{1.25}$$

where $\boldsymbol{\theta} \wedge \mathbf{m} = \theta_1 m_2 - \theta_2 m_1$, and $q_{\mathrm{f}}(\mathbf{m})$ is the first component of $\mathbf{z}_{\mathrm{f}}$ as defined in (1.24). The term independent of $\boldsymbol{\theta}$ on the right hand side of (1.25) is just the classical action of the periodic orbit containing the fixed point labelled $\mathbf{m}$. The amplitude factor in front of the exponential is determined by the stability of this orbit. Specifically,

$$R_{\mathbf{m}}^{(k)} = 2 - \operatorname{Tr}(\mathcal{M}_{\mathbf{m}}^k), \tag{1.26}$$

where $\mathcal{M}_{\mathbf{m}}$ is the monodromy matrix, that is, the map $\boldsymbol{\phi}$ linearized about the fixed point labelled $\mathbf{m}$. We outline a derivation of (1.23) in appendix A. For the cat maps, the trace formula is an identity, rather than a semiclassical approximation [26].

8

The physical origin of the term $\boldsymbol{\theta} \wedge \mathbf{m}$ is as follows. The integers m_1 and m_2 are the number of times that the torus is wound around in the two fundamental directions after k iterations of the map $\boldsymbol{\phi}$. Therefore, this term accounts semiclassically for the periodicity properties (1.17). It is this contribution which is responsible for the COE $\rightarrow$ CUE transition.

Let us suppose that the unperturbed map A and its perturbation $P(q, p)$ are both invariant under time-reversal T. Then $\boldsymbol{\phi}$ will be invariant under the anticanonical symmetry $T \circ P(q, p)$. The Anosov map described above has this property. The classical actions associated with a fixed point $\mathbf{m}$ and its time-reversed[1] partner $\mathbf{m}^*$ are equal. Therefore, if we quantize $\boldsymbol{\phi}$ with periodic boundary conditions, $NS_{\boldsymbol{\phi}^k}(\mathbf{m}^*, \mathbf{0}) = NS_{\boldsymbol{\phi}^k}(\mathbf{m}, \mathbf{0})$ mod 1. Because we have chosen a map with no other symmetry, there is typically no further degeneracy among the actions and we expect that the spectral statistics should be COE [5]. However, for some values of $\boldsymbol{\theta} \neq \mathbf{0}$ the action associated with $\mathbf{m}$ might differ from that associated with $\mathbf{m}^*$. In this case there would be no degeneracy left among the actions and we would expect a transition to CUE statistics. Therefore, we must determine the values of $\boldsymbol{\theta}$ such that

$$NS_{\boldsymbol{\phi}^k}(\mathbf{m}^*, \boldsymbol{\theta}) \neq NS_{\boldsymbol{\phi}^k}(\mathbf{m}, \boldsymbol{\theta}) \text{ mod 1}. \tag{1.27}$$

In appendix B we show that (1.27) holds if

$$T \cdot \boldsymbol{\theta} \neq \boldsymbol{\theta} \text{ mod 1}. \tag{1.28}$$

We note that the above arguments can be generalised. Any canonical torus map [28] can be expressed as the composition of an element of $SL(2, \mathbb{Z})$ with a map which commutes with lattice translations, *i.e.* such that $P(\mathbf{z} + \mathbf{m}) = P(\mathbf{z}) + \mathbf{m}$. So if $\boldsymbol{\phi}$ has a symmetry $\boldsymbol{\gamma}$ (canonical or anticanonical), it will be of the form $\boldsymbol{\gamma} = C \circ P$, where C is linear. This symmetry will cause a degeneracy among the classical actions. Such a degeneracy will be broken in (1.25) if $C \cdot \boldsymbol{\theta} \neq \boldsymbol{\theta}$ mod 1, and therefore we may expect different statistics according to the boundary conditions chosen for the quantization.

It is worth remrking that the condition (1.28) is analogous to that which determines the spectral statistics of Aharonov-Bohm billiards. In that case, time-reversal corresponds to reversing the sign of the magnetic field, and so changing the sign of the flux. But the Aharonov-Bohm effect is periodic in the flux with period one, in appropriate units. So when the flux is zero or 1/2 (the fixed points of sign-reversal modulo 1), quantum mechanics should be time-reversal invariant (assuming the classical mechanics is too), but not otherwise. For zero flux this is obvious. When the flux takes the value 1/2, it is the 'false time-reversal symmetry breaking' of [8].

The fixed points of time-reversal (1.6) are

$$\boldsymbol{\theta} = (\theta, 0) \quad \text{and} \quad \boldsymbol{\theta} = (\theta, 1/2) \tag{1.29}$$

where θ can assume any value. Consider the map (1.7) perturbed with the shear in momentum (1.10); based on the above arguments, we should expect COE statistics if $\boldsymbol{\theta}$

---

[1]Here and in what follows, we shall generically use the term 'time-reversed' to address the properties of the orbit $T \circ P(\mathbf{z}_{\mathrm{f}})$, where $T \circ P$ can be any anticanonical map. This will be done when there is no risk of confusion. When we have to distinguish between time-reversal and other anticanonical symmetries, it will be clearly specified by the context.

assumes one of the values (1.29), and CUE otherwise. In Figure 5 we show the eigenvalue distributions of ϕ quantized with $\boldsymbol{\theta} = (1/6, 5/6)$. The statistics are COE, not CUE. In fact, we find COE statistics for all allowed $\boldsymbol{\theta}$.

[Figure 5 about here.]

Let us now perturb the map (1.7) with the composition of two shears (1.15) as in Section 1.1. Since time-reversal is a symmetry of A, $A \circ P_p \circ P_q$ will be invariant under $T \circ P_p \circ P_q$. As in Section 1.1, $A \circ P_p \circ P_q$ and $A \circ P_p$ have the same symmetries, therefore we expect the same statistics. In Figure 6 the statistics of $A \circ P_p \circ P_q$, quantized with the same boundary condition as $A \circ P_p$, are plotted. This time the eigenvalue distributions are consistent with the expected CUE form.

[Figure 6 about here.]

Here, as in the example of Section 1.1, the cat map perturbed with just one shear has an antiunitary symmetry which the second perturbation destroys. Nevertheless, the symmetry properties of the classical dynamics are the same for both maps, and so cannot account for the statistics observed.

2   Pseudo-symmetries

The quantum Wigner functions for any torus map are kinematically constrained to have support at points on a lattice, which we shall call the *Wigner lattice*. The quantum mechanics of a cat map A then corresponds, up to a phase factor, to the (classical) dynamics it generates on the Wigner lattice. Therefore, to each quantum symmetry there corresponds a symmetry of the classical dynamics on this quantum lattice.

There are matrices which are symmetries of A on the Wigner lattice, but which do not commute with A when they act on other points in phase space. These are discussed in Section 2.1, and then used in Section 2.2 to construct symmetries of the quantum map associated with A, and of the quantum maps associated with the nonlinear perturbations of A, which do not have a classical limit. These are responsible for the anomalous statistics discussed in Section 1.1. We address the case of general boundary conditions in Section 2.3.

2.1   Lattice symmetries

The Wigner function for a pure quantum state is a real function on phase space, defined in conventional units by

$$W(q, p) = \frac{1}{\hbar\pi} \int_{-\infty}^{\infty} dq' \psi(q + q') \psi^*(q - q') e^{-i2q'p/\hbar}. \tag{2.1}$$

It is the analogue of a classical phase space distribution, in the sense that its projections onto the q and p axes are the position and momentum probability densities $|\psi(q)|^2$ and $\left|\tilde{\psi}(p)\right|^2$ respectively.

10

For systems whose classical phase space is the two-torus, $W(q,p)$ is kinematically constrained to be of the form

$$W(q,p) = \sum_{j,k=1}^{2N} c_{jk}\, \delta_{\mathbb{S}^1}(q - j/2N - \theta_1/N)\delta_{\mathbb{S}^1}(p - k/2N - \theta_2/N), \qquad (2.2)$$

where $\delta_{\mathbb{S}^1}(x)$ is the delta function on the circle and the coefficients c_{ij} are such that

$$\begin{aligned} c_{jk} &= (-1)^{2N(p-\theta_2/N)}c_{j+N\,k} = (-1)^{2N(q-\theta_1/N)}c_{j\,k+N} \\ &= c_{j+N\,k+N}(-1)^{[2(p-\theta_2/N)+2(q-\theta_1/N)+1]N}. \end{aligned} \qquad (2.3)$$

That is, W has support on a lattice of points, the *Wigner lattice*, related to $N = 1/h$ and the boundary phases $\boldsymbol{\theta}$.

The Wigner function has a property that is fundamental to our purposes: when the quantum dynamics is determined by a unitary transformation corresponding to a linear map, the Wigner function itself maps classically on the Wigner lattice [23].

To begin with, let us consider the case when $\boldsymbol{\theta} = \mathbf{0}$. The support of the Wigner functions is then the lattice of rational points with denominators $2N$. Such a lattice is invariant under the action of A. If now $A = \bar{A}$ mod $2N$, we have that

$$W(A \cdot \mathbf{z}) = W(\bar{A} \cdot \mathbf{z}), \qquad (2.4)$$

since $W(q,p)$ maps classically. Hence

$$U_A = e^{i\phi}U_{\bar{A}}, \qquad (2.5)$$

where U_A denotes the quantum map associated with A. That is, the dynamics generated by the classical map on the Wigner lattice determines the quantum map U up to a phase factor.

Consider now two cat maps A and B which commute modulo $2N$,

$$AB = BA \text{ mod } 2N. \qquad (2.6)$$

This implies that A and B commute on the Wigner lattice, therefore

$$W(AB \cdot \mathbf{z}) = W(BA \cdot \mathbf{z}), \qquad (2.7)$$

and hence

$$U_A U_B = e^{i\phi}\, U_B U_A. \qquad (2.8)$$

In general there exist many solutions (of the order of N) to Equation (2.6). If furthermore $e^{i\phi} = 1$, U_B is a symmetry of U_A even if A and B do not commute. Unitary symmetries of this kind have also been used by Kurlberg and Rudnick [30] in their study of the quantum ergodicity of the cat maps. They are the analogues of the Hecke operators for arithmetics surfaces of constant negative curvature (for a review see [10]). Clearly they do not have a classical limit, because the matrices from which they are constructed depend on N. In other words, (2.6) is a quantum condition on the classical maps.

Just as the Hecke operators are responsible for the non-generic spectral statistics of the eigenvalues of the Laplacian on arithmetic surfaces, so these symmetries of the quantum cat maps may be viewed as the reason why the spectral statistics are non-generic in this case too. For example, they give rise to the exponentially large degeneracies amongst the periodic orbit contributions to the trace formula demonstrated in [26]. Loosely speaking, the spectrum would have to be desymmetrized with respect to all of them before one could hope to see random-matrix behaviour.

More importantly for us here, anticanonical symmetries can be dealt with in a similar way. Every anticanonical map L can be written as the product $\bar{L}T$, where T is time reversal and $\bar{L} = LT$ is canonical. Now,

$$AL = LA^{-1} \bmod 2N \tag{2.9a}$$

$$A\bar{L}T = \bar{L}TA^{-1} = \bar{L}\tilde{A}^{-1}T \bmod 2N, \tag{2.9b}$$

where $\tilde{A}$ denotes the matrix

$$\tilde{A} = TAT. \tag{2.10}$$

By Equation (2.9b) we have

$$A\bar{L} = \bar{L}\tilde{A}^{-1} \bmod 2N. \tag{2.11}$$

Therefore, by (2.5)

$$U_A U_{\bar{L}} = e^{i\phi}\, U_{\bar{L}} U_{\tilde{A}^{-1}}. \tag{2.12}$$

The quantization of T is the complex conjugation operator K in the position representation. Finally, since $U_{\tilde{A}^{-1}}^* = U_{A^{-1}}$, we have that

$$U_A U_L = e^{i\phi}\, U_L U_A^{-1}, \tag{2.13}$$

where $U_L = U_{\bar{L}}K$ is an antiunitary operator.

When $\boldsymbol{\theta} = 0$, there exists a general formula for the phase factor $e^{i\phi}$ in equation (2.5). The congruence $A \equiv \bar{A} \bmod 2N$ can be written

$$A = \bar{A}\left(I + 2N\bar{A}^{-1}M\right) \tag{2.14}$$

where M is an integer matrix. Let us set

$$D = \left(I + 2N\bar{A}^{-1}M\right). \tag{2.15}$$

Then

$$\exp(i\phi) = \binom{D_{12}/N}{D_{11}} \exp\left[\frac{i\pi}{4}\left(D_{11} - 1\right)\right], \tag{2.16}$$

where $\binom{a}{b}$ is the Jacobi symbol. In appendix C we give a derivation of this result.

When $\boldsymbol{\theta} \neq \boldsymbol{0}$ the arguments follow a similar line. For simplicity, we shall consider maps such that $AA^T = I \bmod 2$. The Wigner lattice still contains $2N \times 2N$ points, but

they no longer have rational coordinates with denominator $2N$; they are a sublattice of the points with denominator $s = [2N, Ns_1, Ns_2]$, where s_1 and s_2 are the denominators of θ_1 and θ_2 respectively, and the symbol $[\ldots]$ denotes the least common multiple of its arguments. The relation

$$A \cdot \boldsymbol{\theta} = \boldsymbol{\theta} \bmod 1 \tag{2.17}$$

guarantees that this sublattice is invariant under the action of A. Therefore, for general boundary conditions, (2.8) holds if

$$AB = BA \bmod s \tag{2.18}$$

and

$$B \cdot \boldsymbol{\theta} = \boldsymbol{\theta} \bmod 1. \tag{2.19}$$

The above discussion has important consequences. The main one is that to each symmetry of the quantum cat maps there corresponds a symmetry of the classical dynamics on the Wigner lattice. The reverse might not be true because of the phase factor in (2.8). There are symmetries of the classical dynamics on the Wigner lattice, but not off it, which have exact quantum counterparts. However, if a linear map is not defined on the Wigner lattice it cannot be quantized. The condition (1.28), which was derived semiclassically in Section 1.2, has exactly this meaning. When $T \cdot \boldsymbol{\theta} \neq \boldsymbol{\theta}$, time-reversal does not leave the Wigner lattice invariant and therefore cannot have a quantum counterpart. The quantum symmetry is 'broken'. This is a quantum explanation of the result obtained in the previous section using semiclassical arguments. In Section 2.3 we give other examples of these symmetries.

We are now in a position to understand how the puzzles described in Sections 1.1 and 1.2 might be resolved. Let us consider again the map (1.12). Equation (2.9a) has in general many solutions, even if it is not solvable when we drop the condition $\bmod \, 2N$. If one of these solutions is a symmetry of the shear in momentum $P_p(q, p)$, then U_ϕ will have an antiunitary symmetry and the statistics will be COE, as observed in Figure 3. If furthermore this solution is not a symmetry of the shear in position $P_q(q, p)$ then the introduction of the second shear will destroy the antiunitary symmetry of U_ϕ and the statistics will be CUE, as seen in Figure 4. We will demonstrate that this is indeed the case in Section 2.2. Likewise, when $\boldsymbol{\theta} \neq \mathbf{0}$ we expect an analogous situation to hold, and this is shown to be the case in Section 2.3. It is worth noting that the Wigner lattice is not invariant under nonlinear maps $\boldsymbol{\phi}$, and that then $W(q, p)$ does not map classically. Therefore, quantum symmetries of U_ϕ do not have any link with the dynamics of $\boldsymbol{\phi}$, even on lattices, except in the case of linear maps.

It is also worth noting that in the above arguments we have implicitly assumed that

$$U_{AB} = U_A U_B. \tag{2.20}$$

In general, such a multiplicativity property may be expected to hold only up to a phase factor (see [30]). However, in the Hannay-Berry quantization scheme it holds exactly [23].

Kurlberg and Rudnick [30] developed a quantization scheme when $\boldsymbol{\theta} = \mathbf{0}$ in which U_A depends only on the reduction of $A \bmod 2N$. Their goal was to study the eigenfunctions

of the cat maps and to show that in the semiclassical limit they become equidistributed with respect to Liouville measure. They proved that the multiplicativity property (2.20) always holds if $A = I$ mod 4 when N is even, and $A = I$ mod 2 when N is odd. Unfortunately this constraint considerably limits the class of maps that can be quantized; the maps that we have used do not belong to this class. Moreover, the quantization scheme used in [30] is not equivalent to Hannay and Berry's, in which congruence modulo $2N$ implies equality of the quantum maps only up to a phase factor.

2.2 Quantum symmetries: $\boldsymbol{\theta = 0}$

We now proceed to construct the antiunitary operators which account for the statistics observed in Section 1.1. We begin, in this section, by considering periodic boundary conditions, so that $\boldsymbol{\theta = 0}$. The generalization to other boundary conditions will be made in Section 2.3.

Our strategy, as explained in the previous section, is to find an anticanonical map which is a symmetry of, for example, (1.12) modulo $2N$ and also a symmetry of the nonlinear shear in momentum (1.10). Then the map $\boldsymbol{\phi}$ will not have any classical symmetries, but, as long as the phase factor in (2.13) is one, the corresponding quantum map will. This will then explain the COE statistics seen in Figure 3. Moreover, if this anticanonical matrix is not a symmetry of the shear in position (1.13), the quantum map corresponding to (1.16) will not possess any symmetries. This will, in turn, account for the CUE statistics observed in Figure 4.

We shall consider cat maps with no anticanonical symmetries:

$$A = \begin{pmatrix} a & b \\ c & d \end{pmatrix}, \tag{2.21}$$

with $a \neq d$ (otherwise the map would be time-reversal invariant [26]). As an ansatz for the anticanonical map, we take

$$L(s) = \begin{pmatrix} 1 & 0 \\ m(s) & -1 \end{pmatrix}, \tag{2.22}$$

which is a symmetry of $P_p(q, p)$ but not of $P_q(q, p)$. Our aim is then to find those integers $m(s)$ for which

$$A \cdot L(s) = L(s) \cdot A^{-1} \text{ mod } s. \tag{2.23}$$

A solution to the above equation is given by

$$m(s) = (d - a)(b \backslash s) \text{ mod } s \tag{2.24}$$

where $(b \backslash s)$ is the integer inverse of b with respect to the mutually coprime integer s, $i.e.$ the unique integer modulo s such that $b(b \backslash s) \equiv 1$ mod s. According to the Euler-Fermat theorem

$$s^{\phi(b)} \equiv 1 \text{ mod } b, \tag{2.25}$$

14

where $\phi(b)$ is Euler's function, defined as the number of integers mutually prime and less than b. Hence

$$m(s) = (d-a)\frac{1-s^{\phi(b)}}{b} \bmod s. \tag{2.26}$$

We therefore have a family of lattice symmetries whose only constraint is that b should be coprime with s. These maps determine degeneracies among the contributions to the trace formula from the periodic orbits of $\phi = A \circ P_p(q,p)$ even though ϕ does not have any symmetry. Setting $s = 2N$, we have

$$m(2N) = (d-a)\frac{1-N^{\phi(b)}}{b} \bmod 2N, \tag{2.27}$$

where we have used the fact that $2^{\phi(b)} \equiv 1 \bmod b$ and, since $AA^T = I \bmod 2$, $(d-a)$ is always even. If b is even, we can also reduce $m(2N)$ to the form (2.27); therefore, the only constraint is that b should be coprime to N.

We now show that

$$U_A U_{L(2N)} = U_{L(2N)} U_A^{-1}, \tag{2.28}$$

that is, that the phase factor in (2.13) is one. This can be done by checking that the matrix $U_A U_{\bar{L}(2N)}$, where $\bar{L}(2N) = L(2N)T$, is symmetric.

The matrix elements of $U_{\bar{L}(2N)}$ are

$$\left(U_{\bar{L}(2N)}\right)_{kj} = \exp(i\pi m\,(2N)\,j^2/N)\delta_{kj}. \tag{2.29}$$

The quantum map associated with A is

$$
\begin{aligned}
(U_A)_{kj} = \left(\frac{b}{iN}\right)^{\frac{1}{2}} &\exp\left[\frac{i\pi}{Nb}\left(aj^2 - 2jk + dk^2\right)\right] \\
&\times \left\langle \exp\left\{\frac{i\pi}{b}\left[Nan^2 + 2\left(aj-k\right)n\right]\right\}\right\rangle_n.
\end{aligned}
\tag{2.30}
$$

It can be checked by direct substitution that the multiplicativity property (2.20) is satisfied in this case.

We consider the case when b is odd; the case when b is even can be treated in the same way. The average over n in (2.30) is a Gauss sum and can be evaluated to be

$$\frac{1}{\sqrt{b}}\binom{Na}{b}\exp\left[-\frac{i\pi}{4}(b-1)\right]\exp\left[-i\pi\frac{Na}{b}\left(Na\backslash b\right)^2 \left(aj-k\right)^2\right], \tag{2.31}$$

where $\binom{Na}{b}$ is the Jacobi symbol. The condition on the determinant implies that $(a\backslash b) = d$. Moreover, using the Euler-Fermat theorem, the numerator in the argument of the exponential in (2.31) is

$$-N^{\phi(b)-1}(aj^2 - 2jk + dk^2) \bmod 2b. \tag{2.32}$$

Then

$$(U_A)_{kj} = \frac{1}{\sqrt{N}} \binom{Na}{b} \exp\left(-\frac{i\pi}{4}b\right)$$
$$\times \exp\left[\frac{i\pi}{Nb}\left(1 - N^{\phi(b)}\right)\left(aj^2 - 2jk + dk^2\right)\right]. \quad (2.33)$$

Finally, multiplying the above matrix by (2.29) and using (2.27) we obtain

$$\left(U_A U_{\bar{L}(2N)}\right)_{kj} = \frac{1}{\sqrt{N}} \binom{Na}{b} \exp\left(-\frac{i\pi}{4}b\right)$$
$$\times \exp\left\{\frac{i\pi}{Nb}\left(1 - N^{\phi(b)}\right)\left[d(j^2 + k^2) - 2jk\right]\right\}, \quad (2.34)$$

which is symmetric in j and k.

It is worth noting that we did not explicitly use the hypothesis that A does not have any anticanonical symmetry, but only the fact that the two diagonal elements are different. If A had an anticanonical symmetry, then we would know a priori that U_A has an antiunitary symmetry.

We also remark that if we had considered a shear in position instead of in momentum, we would have obtained analogous results. The problem is symmetric in q and p, as it should be.

Finally, we point out the following generalization of the perturbations used above. Consider a cat map which does not have any anticanonical symmetries. The only condition required on the momentum shear for our analysis to hold unchanged is that it breaks parity, so that the classical dynamics will not have any canonical symmetries. The most general form of $F(q)$ is

$$F(q) = \sum_{k=1}^{\infty} \left(a_k \sin 2\pi kq + b_k \cos 2\pi kq\right). \quad (2.35)$$

In order to break parity, there must be at least one nonzero b_k. Any choice of $F(q)$ for which this is the case will lead to COE spectral statistics. The Fourier coefficients can be thought of as arbitrary parameters, and so we can construct families of systems depending continuously upon any given number of parameters whose classical dynamics are not time reversal invariant but whose quantum spectral statistics are those of the COE; that is, for which the corresponding quantum maps possess antiunitary symmetries that do not have a classical limit and which lead to 'paradoxical' statistics.

2.3   Quantum symmetries: $\boldsymbol{\theta \neq 0}$

We now extend the theory developed in the previous section to cat maps which are time reversal invariant and quantized for any allowed boundary conditions $\boldsymbol{\theta}$. The purpose is to explain the statistics shown in Figures 5 and 6. We shall see that whichever cat map and boundary conditions we choose, a perturbation by a single shear in either position or momentum leads to spectral statistics that are COE, irrespective of the symmetries of the classical dynamics. The causes are again quantum symmetries which do not have a classical limit.

16

The problem for general $\boldsymbol{\theta}$ could be approached by following the same lines as the previous section, that is by looking for an anticanonical map of the form (2.22). The mathematics would be more involved, but the underlying ideas would be the same. However, $L(s, \boldsymbol{\theta})$ must obey the condition (2.17), which is equivalent to solving the equation

$$m(s)\theta_1 = 2\theta_2 \text{ mod } 1. \tag{2.36}$$

θ_1 and θ_2 are rationals, and so (2.36) may not have solutions in $\mathbb{Z}$. Therefore, this approach would not work in every case.

The construction that we now give works for any allowed boundary conditions. We shall consider linear maps which are time-reversal invariant, *i.e.* such that $a = d$ in (2.21). As before, we shall also require b to be coprime with N.

First, we need an expression for $\boldsymbol{\theta}$ in terms of the matrix elements of A. Without loss of generality we take $b < c$. Using the condition on the determinant and (2.17) we obtain

$$\begin{pmatrix} \theta_1 \\ \theta_2 \end{pmatrix} = -\frac{1}{2} \begin{pmatrix} 1 & -\frac{b}{a-1} \\ -\frac{a+1}{b} & 1 \end{pmatrix} \begin{pmatrix} v \\ w \end{pmatrix}, \tag{2.37}$$

where v and w are integers.

The Wigner function behaves under translations in the same way as when the wavefunction is propagated by linear transformations: it maps classically. The quantum translation operator in momentum is $T_p(z) = e^{\frac{iz}{\hbar}\hat{q}}$. Using the definition of the Wigner function (2.1) it is straightforward to see that if the wavefunction is propagated by $T_p(z)$, then the Wigner function is given by $W(q, p+z)$. This has the same consequences as for the cat maps: if the classical translation commutes with A modulo $s = [2N, Ns_1, Ns_2]$, where s_1 and s_2 are the denominators of θ_1 and θ_2 respectively, then $T_p(z)$ commutes with U_A up to a phase factor.

Consider the anticanonical map

$$B(\boldsymbol{\theta}, N)(q, p) = (q, -p + 2N^{\phi(b)-1}\theta_2). \tag{2.38}$$

By (2.37), the denominator of θ_2 is a factor of $2b$, therefore the map (2.38) is a composition of translation in p by $2\theta_2/N + \omega/N$, where ω is an integer, and time-reversal. The translation

$$\tau(N, \boldsymbol{\theta})(q, p) = (q, p + 2N^{\phi(b)-1}\theta_2) \tag{2.39}$$

does not have a quantum counterpart in $\mathcal{H}(\boldsymbol{\theta})$, as the only admissible quantum translations for torus maps are multiples of Planck's constant $1/N$ [28]. However, the composition $B(N, \boldsymbol{\theta}) = \tau(N, \boldsymbol{\theta}) \circ T$ leaves the Wigner lattice invariant and is well defined in $\mathcal{H}(\boldsymbol{\theta})$. The map (2.38) is an exact symmetry of A, not only a symmetry modulo $s = [2N, Ns_1, Ns_2]$. It is also a symmetry of $P_p(q, p)$ but not of the shear in position $P_q(q, p)$.

In appendix D we show that the matrix

$$U_A \circ T_p(2N^{\phi(b)-1}\theta_2) \tag{2.40}$$

is symmetric and therefore $T_p(2N^{\phi(b)-1}\theta_2) \circ U_T$ is a symmetry of U_A.

There exists a whole family of distinct classical symmetries of A, each of which corresponds to a choice of N coprime to b. They are also symmetries of $P_p(q, p)$. However, we do not see their effect in the spectral statistics of the Anosov perturbations because most of them do not have quantum counterparts. If they had we would observe degeneracy in the spectra instead of RMT statistics. For example, suppose that we quantize $\phi = A \circ P_p(q, p)$ with periodic boundary conditions, and that A is time-reversal invariant. Then all the translations $\tau(\boldsymbol{\theta}, s)$ where s is any integer coprime to b, are canonical symmetries of ϕ. The reason that they cannot be quantized is that they map $\mathcal{H}(\mathbf{0}) \longrightarrow \mathcal{H}(\boldsymbol{\theta})$, where $\boldsymbol{\theta} = (0, \frac{2N}{s}\theta_2 + \frac{N\omega}{s})$. An alternate, more instructive point of view is that none of the maps (2.38) acts on the Wigner lattice for $\boldsymbol{\theta} = \mathbf{0}$, because they are defined only for b coprime to N.

This situation is analogous to the arithmetical symmetries analysed in Section 2.2. In that case we had a whole family of maps leaving A invariant modulo s; they were responsible for the degeneracy among the periodic orbits. One in particular acts on the Wigner lattice and allows the construction of an exact quantum symmetry with no classical limit. Similarly, the quantum symmetries $T_p(2N^{\phi(b)-1}\theta_2) \circ U_T$ do not have a classical limit as the map from which they are constructed depends on N.

Now consider the map whose statistics are shown in Figure 5. It was quantized with $\boldsymbol{\theta} = (1/6, 5/6)$. For these values of the phases time-reversal does not leave the Wigner lattice invariant, but $B(N, \boldsymbol{\theta})$ does and therefore has a quantum counterpart; we observe COE statistics. In Figure 6 the statistics are CUE because $B(N, \boldsymbol{\theta})$ is not a symmetry of the shear in position $P_q(q, p)$.

3   Concluding remarks

We begin by summarizing our main results. The quantum dynamics of linear torus maps corresponds to the action of the classical maps on the Wigner lattice. The arithmetical nature of the linear dynamics on the Wigner lattice has properties which are not inherited by the classical motion on the rest of phase space. Symmetries on the Wigner lattice are symmetries of the corresponding quantum map. These quantum symmetries do not have a classical limit, as the classical maps from which they are constructed depend on N.

In general, cat maps have many arithmetical quantum symmetries, both unitary and antiunitary, which account for the degeneracy of their spectra, and the fact that their spectral statistics are not those of any of the RMT ensembles. When they are perturbed, some of these symmetries may survive and therefore the spectral statistics may not be those expected on the basis of the symmetries of the classical motion. We have studied these arithmetical pseudo-symmetries for cat maps perturbed with shears and quantized with periodic as well as more general boundary conditions. The advantage of using these perturbations is that quantum maps which are not merely semiclassical approximations can be obtained easily and therefore they are particularly suited to investigating symmetries whose nature is purely quantum mechanical.

When a cat map is quantized with one shear in either position or momentum, at least one of these arithmetical symmetries always survives, irrespective of the classical symmetries of the unperturbed map and of the boundary conditions used. Therefore, the statistics are COE. When the map is perturbed with two orthogonal shears these

symmetries are broken and the statistics are then CUE, if the cat map itself has no anticanonical symmetries.

This behaviour poses interesting problems for attempts to develop a general semiclassical theory of spectral statistics. The idea behind semiclassical theories is to determine quantum quantities in terms of classical objects as $\hbar \to 0$. In this spirit, spectral statistics should be related to statistical measures of classical chaos, like ergodicity or mixing. But, as we have shown, pseudo-symmetries affect the spectral statistics and yet have no classical interpretation. It is true that they give rise to degeneracies among the periodic orbit contributions to the trace formula, but such degeneracies do not have an explanation in terms of the classical dynamics. Moreover, calculating all of the classical periodic orbits is in principle equivalent (via the trace formula) to calculating all the quantum eigenvalues, and the aim of semiclassical theories is to determine eigenvalue correlations without having to do this.

In practice, these degeneracies can, of course, be seen from a finite number of orbits, and thus there is always a semiclassical *algorithm* for determining the spectral statistics. But this does not represent to our minds a satisfactory semiclassical *theory*. Such a theory would, in our opinion, require that, in the semiclassical limit, spectral statistics could be predicted without having to compute any periodic orbits, being instead determined by symmetries and universal statistical properties of the long-time classical dynamics.

Geodesic motion on arithmetic surfaces on constant negative curvature and the cat maps are examples of maximally chaotic systems which do not fall in the universality classes of the RMT conjecture. Since these are isolated systems their behaviour has, in the past, been termed 'non-generic'. However, even though the Anosov maps discussed here are not counter-examples to the RMT conjecture — the arithmetical symmetries derived in Section 2 explain their statistics — their spectral distributions cannot be interpreted in terms of classical quantities. Moreover, they are not isolated: families can be constructed which depend continuously on any given number of parameters. Therefore, they provide further evidence of the difficulty of constructing a general semiclassical proof of the random-matrix conjecture.

From this point of view, it would be interesting to know if families of perturbations of arithmetical billiards could be constructed which preserve some of their non-classical (Hecke) symmetries in the same way.

The pseudo-symmetries described here should not be considered only for the problems they pose; they can also play a constructive role in explaining the quantum properties of torus maps. For example, Kurlberg and Rudnick [30] used them in their investigation of quantum ergodicity for the cat maps. It also seems possible that they might form the basis of a much deeper, rigorous understanding of at least the long-range spectral statistics of the cat maps, in the same way as for arithmetical billiards [10].

Acknowledgements

A Trace formula for Anosov maps

We here give a derivation of the trace formula (1.23). The trace formula for the cat maps quantized with $\boldsymbol{\theta} = \mathbf{0}$ was calculated in [26]. In this appendix we generalize that derivation to nonlinear Anosov maps sufficiently close to a cat map and to general boundary conditions.

The semiclassical propagator for one dimensional systems is given in conventional units by

$$\langle q_2| U |q_1\rangle \simeq \left(\frac{i \, \partial^2 S}{h \, \partial q_1 \partial q_2} \right)^{1/2} \exp\left[iS\left(q_2, q_1 \right)/\hbar \right]. \tag{A.1}$$

Each power k of the map

$$\boldsymbol{\phi} = A \circ P(\mathbf{z}), \tag{A.2}$$

where $P(\mathbf{z})$ represents a general perturbation, can be written as the product of A^k times a map $P^{(k)}(\mathbf{z})$ which commutes with lattice translations [28]. If $P(\mathbf{z})$ satisfies Anosov's theorem, then so will $P^{(k)}(\mathbf{z})$ for every k. Therefore the generating function of $\boldsymbol{\phi}^k$ to be inserted in (A.1) will be

$$S_{\boldsymbol{\phi}^k}(q_2, q_1) = S_{A^k}(q_2, q_i) + S_{P^{(k)}}(q_i, q_1), \tag{A.3}$$

where $q_i(q_1, q_2)$ is the intermediate coordinate after the action of $P^{(k)}$.

The generating function $S_{P^{(k)}}(q_i, q_1)$ will in general be very complicated, but, together with its derivatives, satisfies

$$S_{P^{(k)}}(q_2 + m, q_1 + m) = S_{P^{(k)}}(q_2, q_1), \tag{A.4}$$

where m is an integer. This property is a consequence of the fact that $P^{(k)}(\mathbf{z})$ is a time-one flow of a periodic Hamiltonian.

The action $S_{A^k}(q_2, q_i)$ is just

$$S_{A^k}(q_2, q_1) = \frac{1}{2b_k} \left(d_k q_2^2 - 2q_1 q_2 + a_k q_1^2 \right), \tag{A.5}$$

where

$$A^k = \begin{pmatrix} a_k & b_k \\ c_k & d_k \end{pmatrix} \tag{A.6}$$

To obtain the semiclassical map corresponding to $\boldsymbol{\phi}^k$, we insert the action (A.3) into (A.1) and average over $q_2 + m_1$ [23]. Moreover, the kinematics of torus quantization implies that $q_1 = (j + \theta_1)/N$ and $q_2 = (k + \theta_1)/N$. Thus we have

$$\left(U_{\boldsymbol{\phi}}^k \right)_{kj} \simeq \left\langle \left(\frac{2\pi i N \, \partial^2 S_{\boldsymbol{\phi}^k}}{\partial q_1 \partial q_2} \right)^{1/2} \right. $$
$$\left. \times \exp\left[-2\pi i m_1 \theta_2 + 2\pi i N S_{\boldsymbol{\phi}^k}(q_2 + m_1, q_1) \right] \right\rangle_{m_1}. \tag{A.7}$$

We now take the trace of U_{ϕ}^k and exchange the sum with the average; this is allowed because, as we shall see, they are both finite sums. Then, applying the Poisson summation formula (1.21),

$$
\mathrm{Tr}\left(U_{\phi}^k\right) \simeq \left\langle \sum_{m_2=-\infty}^{\infty} \left(\frac{iN^3 \, \partial^2 S_{\phi^k}}{\partial q_1 \partial q_2}\right)^{1/2} \exp\left(2\pi i \boldsymbol{\theta} \wedge \mathbf{m}\right) \right.
$$
$$
\left. \times \int_{0-\epsilon}^{1-\epsilon} \exp\left[2\pi i N \left(S_{\phi^k}(q+m_1,q) - m_2 q\right)\right] dq \right\rangle_{m_1}.
\tag{A.8}
$$

In order to obtain a trace formula as a sum over periodic orbits, we transform (A.8) from an infinite sum of finite integrals to a finite sum of infinite integrals [9]. We shall then evaluate the integral using the stationary phase approximation.

The intermediate point $q_i(q_2,q_1)$ after the action of $P^{(k)}$ is of the form $q_i = q_1 + \epsilon(q_1,q_2)$, where $\epsilon(q_1,q_2)$ is small; moreover, in the integral (A.8) $q_1 = q_2 = q$,[2] therefore we simply write $q_i = q + \epsilon(q)$. In what follows we shall keep only terms that are $O(\epsilon(q))$. Therefore, the argument of the exponential (A.8) becomes

$$
\boldsymbol{\theta} \wedge \mathbf{m} + N\left[S_{A^k}(q+m_1,q) - m_2 q + S_{P^{(k)}}(q,q)\right.
$$
$$
\left. + \left(\frac{\partial S_{A^k}(q+m_1,q)}{\partial q_1} + \frac{\partial S_{P^{(k)}}(q,q)}{\partial q_2}\right)\epsilon(q)\right]. \tag{A.9}
$$

The term in the brackets involving the derivatives of the actions is zero up to terms of order $O(\epsilon(q))$, because $q = q_i - \epsilon(q_i)$ and

$$
\left.\frac{\partial S_{A^k}(q+m_1,q_i)}{\partial q_1}\right|_{\substack{q_1=q_i \\ q_2=q+m_1}} = -\left.\frac{\partial S_{P^{(k)}}(q_i,q)}{\partial q_2}\right|_{\substack{q_1=q \\ q_2=q_i}}. \tag{A.10}
$$

At order $O(\epsilon(q))$, (A.9) therefore reduces to

$$
\boldsymbol{\theta} \wedge \mathbf{m} + N\left[S_{A^k}(q+m_1,q) - m_2 q + S_{P^{(k)}}(q,q)\right]. \tag{A.11}
$$

The term $S_{A^k}(q + m_1,q) - m_2 q$ is the action of the unperturbed map. In [26] it was shown that this can be written as a sum of two terms: one quadratic in q; the other independent of the variable of integration and invariant under translations by the parallelogram obtained by applying the matrix $(A^k - I)$ to the unit square. Such a parallelogram tessellates the plane and contains the winding numbers associated to all the periodic points with period k. The curvilinear parallelogram introduced in Section 1.2 is obtained by slightly deforming the former and has the same properties because ϕ is topologically conjugate to A. In what follows we do not distinguish between them. In other words, the winding numbers are not changed by the perturbation.

The integral in (A.8) also involves the term $S_{P^{(k)}}(q,q)$, which by (A.4) is periodic. Therefore, the sum over m_2 may be split into contributions from each of the lattice points

---

[2]The point q is not yet required to be on a periodic orbit, so in general $p_1(q) \neq p_2(q)$

in the fundamental parallelogram:

$$\operatorname{Tr}\left(U_{\boldsymbol{\phi}}^{k}\right) \simeq \left\langle \sum_{m_2 \in \square} \left(\frac{i N^3 \, \partial^2 S_{\boldsymbol{\phi}^k}}{\partial q_1 \partial q_2}\right)^{1/2} \exp\left(2\pi i \boldsymbol{\theta} \wedge \mathbf{m}\right) \right.$$
$$\left. \times \int_{-\infty}^{\infty} \exp\left[2\pi i N \left(S_{\boldsymbol{\phi}^k}(q + m_1, q) - m_2 q\right)\right] dq \right\rangle_{m_1}, \quad \text{(A.12)}$$

where the symbol $\square$ denotes the fundamental parallelogram.

Since we are interested in the semiclassical limit $N \to \infty$ we can apply the stationary phase approximation to the above integral:

$$\frac{\partial}{\partial q}\left(S_{\boldsymbol{\phi}^k}(q + m_1, q) - m_2 q\right)$$
$$= \left[\frac{\partial}{\partial q_2} S_{\boldsymbol{\phi}^k}(q_2 + m_1, q_1) + \frac{\partial}{\partial q_1} S_{\boldsymbol{\phi}^k}(q_2 + m_1, q_1) - m_2\right]_{q_2 = q_1 = q}$$
$$= p(q, q) - p(q, q) - m_2 = 0 \bmod 1, \quad \text{(A.13)}$$

that is, q must be a periodic point. We shall denote it by $q_{\mathrm{f}}(\mathbf{m})$, which is related to the lattice points via (1.24). The main contributions to the above integral come from the periodic orbits, which, because of Anosov's theorem, are the same in number as the fixed points of A^k, i.e. $\operatorname{Tr}(A^k) - 2$.

The stationary phase approximation brings an extra factor in front of the exponential in (A.12) which is given by

$$\left(i N \left.\frac{\partial^2 S_{\boldsymbol{\phi}^k}(q + m_1, q)}{\partial q^2}\right|_{q = q_{\mathrm{f}}(\mathbf{m})}\right)^{-1/2}. \quad \text{(A.14)}$$

From the general theory of the trace formula [22] we have that

$$\left.\frac{\partial^2 S_{\boldsymbol{\phi}^k}(q + m_1, q)}{\partial q^2}\right|_{q = q_{\mathrm{f}}(\mathbf{m})} \left/ \left.\frac{\partial^2 S_{\boldsymbol{\phi}^k}(q_2 + m_1, q_1)}{\partial q_1 \partial q_2}\right|_{q_2 = q_1 = q_{\mathrm{f}}(\mathbf{m})} \right.$$
$$= \det\left(\mathcal{M}_{\mathbf{m}}^k - I\right) = 2 - \operatorname{Tr}(\mathcal{M}_{\mathbf{m}}^k) = R_{\mathbf{m}}^{(k)}, \quad \text{(A.15)}$$

where $\mathcal{M}_{\mathbf{m}}^k$ is the monodromy matrix and is related to the stability of the orbit.

(A.12) now becomes

$$\operatorname{Tr}\left(U_{\boldsymbol{\phi}}^{k}\right) \simeq \left\langle \sum_{m_2 \in \square} \frac{-i N}{\sqrt{-R_{\mathbf{m}}^{(k)}}} \exp\left(2\pi i \boldsymbol{\theta} \wedge \mathbf{m}\right) \right.$$
$$\left. \times \exp\left[2\pi i N \left(S_{\boldsymbol{\phi}^k}\left((q_{\mathrm{f}}(\mathbf{m}) + m_1, q_{\mathrm{f}}(\mathbf{m})) - m_2 q_{\mathrm{f}}(\mathbf{m})\right)\right)\right] \right\rangle_{m_1}. \quad \text{(A.16)}$$

The exponential above is periodic under translations by the fundamental parallelogram [26], as are the second derivatives of the action and therefore (A.15) as well. The average is

therefore a finite sum over the integers m_1 which belong to the fundamental parallelogram. Thus we can drop the brackets denoting the average and write (A.16) as a sum over all the lattice points in the fundamental parallelogram, or equivalently over all fixed points of ϕ^k. The trace formula then becomes

$$\text{Tr}\left(U_{\phi}^k\right) \simeq \sum_{\mathbf{m}\in\square} \frac{1}{\sqrt{-R_{\mathbf{m}}^{(k)}}} \exp\left[2\pi i N S_{\phi^k}\left(\mathbf{m},\boldsymbol{\theta}\right)\right], \tag{A.17}$$

where the effective action is

$$S_{\phi^k}(\mathbf{m},\boldsymbol{\theta}) = \boldsymbol{\theta}\wedge\mathbf{m}/N + S_{\phi^k}(q_{\text{f}}(\mathbf{m}) + m_1, q_{\text{f}}(\mathbf{m})) - m_2 q_{\text{f}}(\mathbf{m}). \tag{A.18}$$

B Trace formula and symmetry

Consider the Anosov map $\phi = A \circ P$, where A and P are both time-reversal invariant. Then $T \circ P$ will be a symmetry of ϕ. Suppose furthermore that $AA^T = I$ mod 2, and that the perturbation is chosen so that ϕ does not have any canonical symmetry. Using the trace formula derived in appendix A we now show that

$$N S_{\phi^k}(\mathbf{m}^*,\boldsymbol{\theta}) = N S_{\phi^k}(\mathbf{m},\boldsymbol{\theta}) \text{ mod } 1. \tag{B.1}$$

if

$$T\cdot\boldsymbol{\theta} = \boldsymbol{\theta} \text{ mod } 1. \tag{B.2}$$

Here * denotes the time-reverse orbit. We shall use the same notation as appendix A.

The winding numbers $\mathbf{m}^*$ are easy to find in terms of A, T and $\mathbf{m}$. As pointed out in appendix A, the winding numbers are not changed by the perturbation. Using the definition of anticanonical symmetry (1.3) one has

$$\mathbf{m}^* = -A^k T\cdot\mathbf{m}. \tag{B.3}$$

In order to obtain $S_{\phi^k}(\mathbf{m}^*,\boldsymbol{\theta})$, we need to write the action as an explicit function of $\mathbf{m}$. Up to terms of order $O(\epsilon(q))$, $S_{\phi^k}(\mathbf{m},\boldsymbol{\theta})$ is given by

$$\begin{aligned}
S_{\phi^k}(\mathbf{m},\boldsymbol{\theta}) = \boldsymbol{\theta}\wedge\mathbf{m}/N &+ \Big[S_{A^k}(q_{\text{f}}(\mathbf{m}) + m_1, q_{\text{f}}(\mathbf{m}) - m_2 q_{\text{f}}(\mathbf{m})) \\
&+ S_{P^{(k)}}(q_{\text{f}}(\mathbf{m}), q_{\text{f}}(\mathbf{m})) + \left(\frac{\partial S_{A^k}(q_{\text{f}}(\mathbf{m}) + m_1, q_{\text{f}}(\mathbf{m}))}{\partial q_1}\right. \\
&+ \left.\frac{\partial S_{P^{(k)}}(q_{\text{f}}(\mathbf{m}), q_{\text{f}}(\mathbf{m}))}{\partial q_2}\right) \epsilon(q_{\text{f}})\Big].
\end{aligned} \tag{B.4}$$

Following the same arguments as in appendix A, the term in the round brackets involving the derivatives of the action is zero at order $O(\epsilon(q))$. By rearranging the above expression

we have:

$$
\begin{aligned}
S_{\boldsymbol{\phi}^k}(\mathbf{m}, \boldsymbol{\theta}) &= \boldsymbol{\theta} \wedge \mathbf{m}/N + \frac{1}{2b}\left\{ dm_1^2 - \tilde{R}_{\mathbf{m}}^{(k)} q_{\mathrm{f}}^2(\mathbf{m}) \right. \\
&\quad \left. + 2q_{\mathrm{f}}(\mathbf{m})\left[(d-1)m_1 - bm_2\right]\right\} \\
&\quad + S_{P^{(k)}}(q_{\mathrm{f}}(\mathbf{m}), q_{\mathrm{f}}(\mathbf{m})) + O(\epsilon^2(q)) \\
&= \boldsymbol{\theta} \wedge \mathbf{m} + \frac{N}{2b}\left\{ dm_1^2 + \tilde{R}_{\mathbf{m}}^{(k)} q_{\mathrm{fc}}^2(\mathbf{m}) \right. \\
&\quad \left. + \tilde{R}_{\mathbf{m}}^{(k)}\left[q_{\mathrm{f}}(\mathbf{m}) - q_{\mathrm{fc}}(\mathbf{m})\right]^2 \right\} + S_{P^{(k)}}(q_{\mathrm{f}}(\mathbf{m}), q_{\mathrm{f}}(\mathbf{m})) + O(\epsilon^2(q)) \\
&= S_{A^k}(\mathbf{m}, \boldsymbol{\theta}) + S_{P^{(k)}}(q_{\mathrm{f}}(\mathbf{m}), q_{\mathrm{f}}(\mathbf{m})) + O(\epsilon^2(q)),
\end{aligned}
\tag{B.5}
$$

where $\tilde{R}_{\mathbf{m}}^{(k)} = \mathrm{Tr}(A^k) - 2$, $S_{A^k}(\mathbf{m}, \boldsymbol{\theta})$ is the effective action of the cat map defined in (A.18), and $q_{\mathrm{f}}(\mathbf{m})$ and $q_{\mathrm{fc}}(\mathbf{m})$ are related by

$$
q_{\mathrm{f}}(\mathbf{m}) = q_{\mathrm{fc}}(\mathbf{m}) + \epsilon(q_{\mathrm{fc}}(\mathbf{m})).
\tag{B.6}
$$

We can now determine $S_{\boldsymbol{\phi}^k}(\mathbf{m}^*, \boldsymbol{\theta})$:

$$
S_{\boldsymbol{\phi}^k}(\mathbf{m}^*, \boldsymbol{\theta}) = S_{A^k}(-A^k T \cdot \mathbf{m}, \boldsymbol{\theta}) + S_{P^{(k)}}(q_{\mathrm{f}}^*(\mathbf{m}), q_{\mathrm{f}}^*(\mathbf{m})) + O(\epsilon^2(q)).
\tag{B.7}
$$

First, we have that

$$
S_{P^{(k)}}(q_{\mathrm{f}}^*(\mathbf{m}), q_{\mathrm{f}}^*(\mathbf{m})) = S_{P^{(k)}}(q_{\mathrm{f}}(\mathbf{m}), q_{\mathrm{f}}(\mathbf{m})),
\tag{B.8}
$$

because $P^{(k)}(\mathbf{z})$ is a time-one flow of a periodic Hamiltonian.

In terms of the winding numbers $S_{A^k}(\mathbf{m}, \mathbf{0})$ is given by [26]

$$
S_{A^k}(\mathbf{m}, \mathbf{0}) = -\frac{1}{2\tilde{R}_{\mathbf{m}}^{(k)}}\left[cm_1^2 - bm_2^2 + 2(d-1)m_1 m_2\right].
\tag{B.9}
$$

We now have

$$
NS_{A^k}(-A^k T \cdot \mathbf{m}, \boldsymbol{\theta}) = NS_{A^k}(-T \cdot \mathbf{m}, \boldsymbol{\theta}) \bmod 1.
\tag{B.10}
$$

The above equality can be derived by direct calculations. However, it can also be seen by noting that if $\mathbf{m}$ are the winding numbers of $\mathbf{z}_{\mathrm{fc}}$, then $A^k \cdot \mathbf{m}$ are the winding numbers of $A^{2k} \cdot \mathbf{z}_{\mathrm{fc}} = \mathbf{z}_{\mathrm{fc}} \bmod 1$, and therefore they are equivalent modulo the fundamental parallelogram. Moreover, using the fact that A is symplectic and that $\boldsymbol{\theta}$ is a fixed point of A,

$$
\boldsymbol{\theta} \wedge A^k \cdot \mathbf{m} = A^k \cdot \boldsymbol{\theta} \wedge \mathbf{m} = \boldsymbol{\theta} \wedge \mathbf{m} \bmod 1.
\tag{B.11}
$$

From (B.9) it is straightforward to show that

$$
S_{A^k}(-T \cdot \mathbf{m}, \mathbf{0}) = S_{A^k}(\mathbf{m}, \mathbf{0}).
\tag{B.12}
$$

Finally, up to terms of order $O(\epsilon(q)^2)$ we have

$$
NS_{\boldsymbol{\phi}^k}(\mathbf{m}^*, \boldsymbol{\theta}) = T \cdot \boldsymbol{\theta} \wedge \mathbf{m} + NS_{\boldsymbol{\phi}^k}(\mathbf{m}, \mathbf{0}).
\tag{B.13}
$$

Therefore (B.1) is verified if and only if

$$
T \cdot \boldsymbol{\theta} = \boldsymbol{\theta} \bmod 1.
\tag{B.14}
$$

24

C   Computing $e^{i\phi}$

In this appendix we derive the formula (2.16) for the phase factor $e^{i\phi}$ using a method introduced in [26].

In Section 2.1 we showed that if two matrices A and $\bar{A}$ are congruent modulo $2N$ then

$$A = \bar{A}D, \tag{C.1}$$

where

$$D = \left(I + 2N\bar{A}^{-1}M\right) \tag{C.2}$$

and M is an integer matrix.

The quantization of the matrix D must be the identity up to a phase factor [23]. Since $U_D = Ie^{i\phi}$, the phase is determined by calculating just one matrix element on the diagonal; we here compute $(U_D)_{00}$. Using the general quantization prescription of [23],

$$(U_D)_{00} = \left(\frac{D_{12}}{iN}\right)^{\frac{1}{2}} \left\langle \exp\left(\frac{i\pi N D_{11}}{D_{12}} n^2\right) \right\rangle_n. \tag{C.3}$$

By equation (2.15) D_{12}/N is an even integer, while D_{11} is odd. The average in (C.3) is a Gauss sum, and can then be evaluated explicitly, giving

$$\exp(i\phi) = \binom{D_{12}/N}{D_{11}} \exp\left[\frac{i\pi}{4}\left(D_{11} - 1\right)\right], \tag{C.4}$$

D   Symmetries and general $\boldsymbol{\theta}$

In this appendix we show that the matrix (2.40) is symmetric. The cat map A is assumed time-reversal invariant, *i.e.* $a = d$. For simplicity, we shall carry out the algebra when $AA^T = I$ mod 2, however these calculations generalize directly to any cat map invariant under time-reversal.

When $\boldsymbol{\theta} \neq \boldsymbol{0}$ the matrix elements of U_A are given by

$$
\begin{aligned}
(U_A)_{kj} = \left(\frac{b}{iN}\right)^{\frac{1}{2}} &\exp\left[\frac{i\pi N}{b}\left(aq_1^2 - 2q_1q_2 + dq_2^2\right)\right] \\
&\times \left\langle \exp\left\{\frac{i\pi}{b}\left[Nan^2 + 2\left((aj - k) + (a-1)\theta_1 + b\theta_2\right)n\right]\right\} \right\rangle_n.
\end{aligned}
\tag{D.1}
$$

By (2.17) the term depending on $\boldsymbol{\theta}$ in the above expression is an integer which we denote by r:

$$r = (a-1)\theta_1 + b\theta_2. \tag{D.2}$$

As in Section 2.2, we consider the case when b is odd; when it is even, the arguments are almost the same. The term (D.2) affects only the Gauss sum (2.31) which now becomes

$$\frac{1}{\sqrt{b}}\binom{Na}{b} \exp\left[-\frac{i\pi}{4}(b-1)\right] \exp\left[-\frac{i\pi Na}{b}\left(Na\backslash b\right)^2\left(aj - k + r\right)^2\right]. \tag{D.3}$$

25

Since A is time-reversal invariant, when $\boldsymbol{\theta} = \mathbf{0}$ U_A is a symmetric matrix. However, when $\boldsymbol{\theta} \neq \mathbf{0}$ the term (D.2) makes U_A non-symmetric. This extra contribution to the numerator of the argument of the exponential in (D.3) gives

$$-N^{2\phi(b)-1}a(aj-k)r \equiv -N^{\phi(b)-1}(j-ak)r \bmod b, \tag{D.4}$$

where we have considered only the contributions depending on j and k.

The matrix elements of $T_p(2N^{\phi(b)-1}\theta_2)$ are

$$\left(T_p(2N^{\phi(b)-1}\theta_2)\right)_{kj} = \exp\left[4\pi i N^{\phi(b)-1}\theta_2\left(j+\theta_1\right)\right]\delta_{kj}. \tag{D.5}$$

By (D.2) we have

$$2\theta_2 = \frac{1}{b}\left[-(a-1)\theta_1 + b\theta_2 + r\right] \tag{D.6}$$

If $A \cdot \boldsymbol{\theta} = \boldsymbol{\theta} + \mathbf{r}$, then $A^{-1} \cdot \boldsymbol{\theta} = \boldsymbol{\theta} - A^{-1} \cdot \mathbf{r}$; therefore since the first component of $\mathbf{r}$ is r

$$-(a-1)\theta_1 + b\theta_2 \equiv ar \bmod b. \tag{D.7}$$

Substituting the above equation into (D.6), (D.5) becomes

$$N^{\phi(b)-1}j\left[(a+1)r\right] \bmod b. \tag{D.8}$$

When U_A and $T_p(2N^{\phi(b)-1}\theta_2)$ are multiplied, (D.8) adds to (D.4) which becomes

$$N^{\phi(b)-1}a(j+k)r \bmod b. \tag{D.9}$$

The above expression is symmetric in j and k, therefore the matrix $U_A \circ T_p(2N^{\phi(b)-1}\theta_2)$ is symmetric.

References

[1] D. V. Anosov. Roughness of geodetic flows on compact Riemannian manifolds of negative curvature. *Dokl. Akad. Nauk SSSR*, **145**, 707–709, 1962.

[2] V. I. Arnold and A. Avez. *Ergodic Problems of Classical Mechanics*. W. A. Benjamin Inc., New York, 1968.

[3] M. Baake and J. A. G. Roberts. Reversing symmetry group of $Gl(2,\mathbb{Z})$ and $PGl(2,\mathbb{Z})$ matrices with connections to cat maps and trace maps. *J. Phys. A: Math. Gen.*, **30**, 1549–1573, 1997.

[4] M. Basilio de Matos and A. M. Ozorio de Almeida. Quantization of Anosov maps. *Ann. Phys.*, **237**, 46–65, 1995.

[5] M. V. Berry. Semiclassical theory of spectral rigidity. *Proc. R. Soc. Lond. A*, **400**, 229–251, 1985.

[6] M. V. Berry. Quantum Chaology. *Proc. R. Soc. Lond. A*, **413**, 183–198, 1987.

[7] M. V. Berry, J. P. Keating, and S. Prado. Orbit bifurcations and spectral statistics. *J. Phys. A: Math. Gen.*, **31**, L245–L254, 1998.

[8] M. V. Berry and M. Robnik. Statistics of energy levels without time-reversal symmetry: Aharonov-Bohm chaotic billiards. *J. Phys. A: Math. Gen.*, **19**, 649–668, 1986.

[9] P. A. Boasman and J. P. Keating. Semiclassical asymptotic of perturbed cat maps. *Proc. R. Soc. Lond. A*, **449**, 629–653, 1995.

[10] E. B. Bogomlny, B. Georgeot, M. J. Giannoni, and C. Schmit. Arithmetical chaos. *Phys. Rep.*, **291**, 220–340, 1997.

[11] E. B. Bogomolny and J. P. Keating. Gutzwiller's trace formula and spectral statistics: beyond the diagonal approximation. *Phys. Rev. Lett.*, **77**, 1472–1475, 1996.

[12] O. Bohigas, M. J. Giannoni, and C. Schmit. Characterization of chaotic quantum spectra and universality of level fluctuation laws. *Phys. Rev. Lett.*, **52**, 1–4, 1984.

[13] E. B. Bogomolny, B. Georgeot, M. J. Giannoni, and C. Schmit. Arithmetical Chaos. *Phys. Reports*, **291**, 220–324, 1997.

[14] A. Bouzouina and S. De Bièvre. Ergodicity and the semiclassical limit on the torus. *Comp. Ren. Ser. I-Mathematique*, **321**, 1085–1087, 1995.

[15] A. Bouzouina and S. De Bièvre. Equipartition of the eigenfunctions of quantized ergodic maps on the torus. *Commun. Math. Phys.*, **178**, 83–105, 1996.

[16] A. Bouzouina and S. De Bièvre. Equidistribution of eigenvalues and semi-classical ergodicity of quantized symplectomorphisms of the torus. *Comp. Ren. Ser. I-Mathematique*, **326**, 1021–1024, 1998.

[17] S. De Briève, M. Degli Esposti, and R. Giachetti. Quantization of a class of piecewise affine transformations on the torus. *Commun. Math. Phys.*, **178**, 73–94, 1996.

[18] T. O. de Carvalho, J. P. Keating, and J. M. Robbins. Fluctuations in quantum expectation values for chaotic systems with broken time-reversal symmetry. *J. Phys. A: Math. Gen.*, **31**, 5631–5640, 1998.

[19] M. Degli Esposti. Quantization of the orientation preserving automorphisms of the torus. *Ann. Inst. H. Poincaré*, **58**, 323–341, 1993.

[20] M. Degli Esposti, S. Graffi, and S. Isola. Classical limit of the quantized hyperbolic toral automorphisms. *Commun. Math. Phys.*, **167**, 471–507, 1995.

[21] B. Eckhardt. Exact eigenfunctions for a quantized map. *J. Phys. A: Math. Gen.*, **19**, 1823–1831, 1986.

[22] M. C. Gutzwiller. Periodic orbits and classical quantization conditions. *J. Math. Phys.*, **12**, 343–358, 1971.

[23] J. H. Hannay and M. V. Berry. Quantization of linear maps on the torus — Fresnel diffraction by a periodic grating. *Physica*, **1D**, 267–290, 1980.

[24] J. H. Hannay and A. M. Ozorio de Almeida. Periodic orbits and a correlation function for the semiclassical density of states. *J. Phys. A: Math. Gen.*, **17**, 3429–3440, 1984.

[25] J. P. Keating. Asymptotic properties of the periodic orbits of the cat maps. *Nonlinearity*, **4**, 277–307, 1991.

[26] J. P. Keating. The cat maps: quantum mechanics and classical motion. *Nonlinearity*, **4**, 309–341, 1991.

[27] J. P. Keating and F. Mezzadri. Torus maps, symmetries, and spectral statistics. Proceedings of the Enrico Fermi School "New Directions in Quantum Chaos", Varenna, 20-30 July 1999. In the press.

[28] J. P. Keating, F. Mezzadri, and J. M. Robbins. Quantum boundary conditions for torus maps. *Nonlinearity*, **12**, 579–591, 1999.

[29] S. Knabe. On the quantization of Arnold's cat. *J. Phys. A: Math. Gen.*, **23**, 2013–2025, 1990.

[30] P. Kurlberg and Z. Rudnick. Eigenfunctions of the quantized cat map. Preprint, 1999.

[31] F. Mezzadri. Boundary conditions for torus maps and spectral statistics. PhD thesis, University of Bristol, 1999.

[32] S. Nonnenmacher. Crystal properties of eigenstates of quantum cat maps. *Nonlinearity*, **10**, 1569–1598, 1997.

[33] S. Nonnenmacher and A. Voros. Chaotic eigenfunctions in phase space. *J. Stat. Phys.*, **92**, 431–518, 1998.

[34] S. Zelditch. Index and dynamics of quantized contact transformations. *Ann. Inst. Fourier*, **47**, 305–365, 1997.

List of Figures

(a) Cumulative spacing distribution for the quantum map corresponding to $A = (10, 3; 33, 10)$. Parity $= +1$ and $N = 1209$.


(b) Number variance for the quantum map corresponding to $A = (10, 3; 33, 10)$. Parity $= +1$ and $N = 1209$.

Figure 1: The cumulative spacing distribution and number variance for the quantum map corresponding to $A = (10, 3; 33, 10)$. The eigenvalues correspond to states with the same parity. The data, solid curves, do not follow the predictions of RMT. The dot-dashed curves are the COE statistics, the dashed curves the CUE.
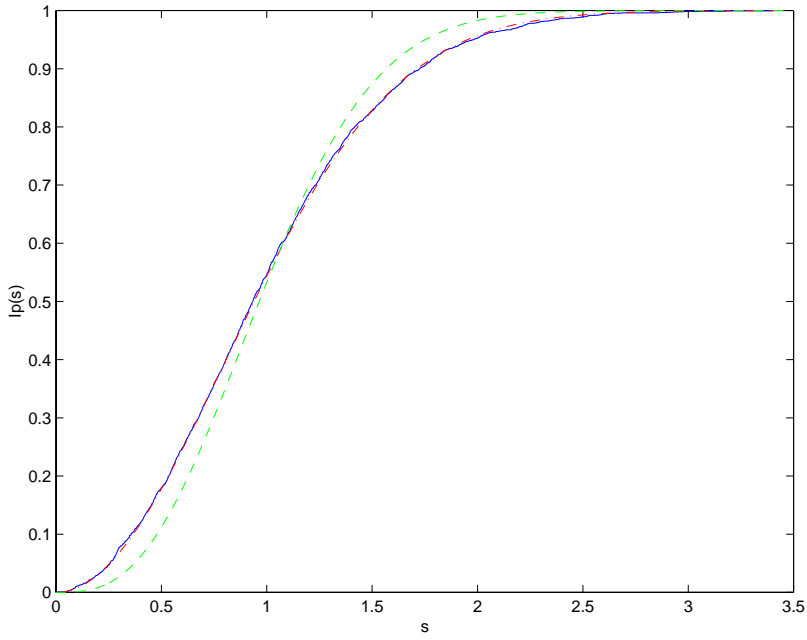
(a) Cumulative spacing distribution for the map (10,3;33,10) perturbed with a shear in momentum. $N = 2417$.
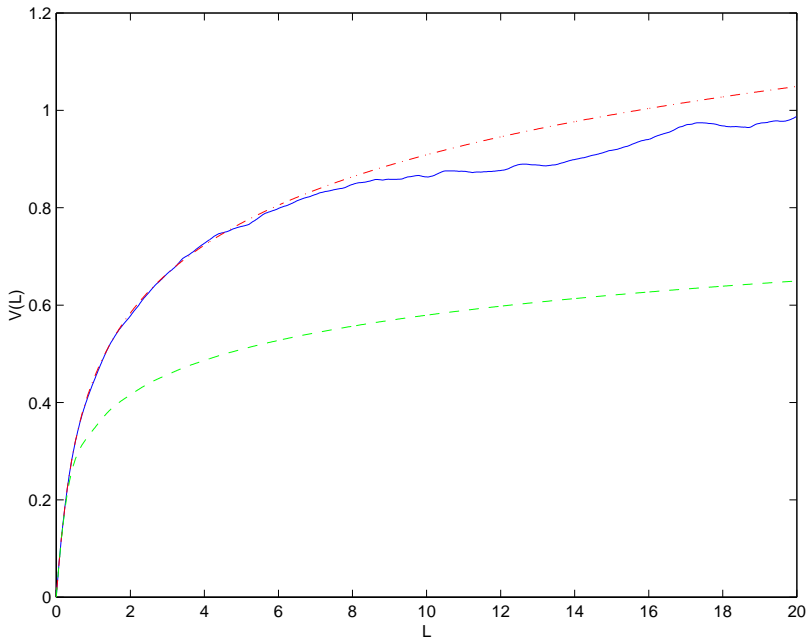
(b) Number variance for the map (10,3;33,10) perturbed with a shear in momentum. $N = 2417$.

Figure 2: The cumulative spacing distribution and number variance for the map $(10, 3; 33, 10)$ perturbed by (1.10) with $k_p = 0.03$. The data, solid curves, follow the COE predictions (dot-dashed curves). The dashed curves are the CUE statistics.
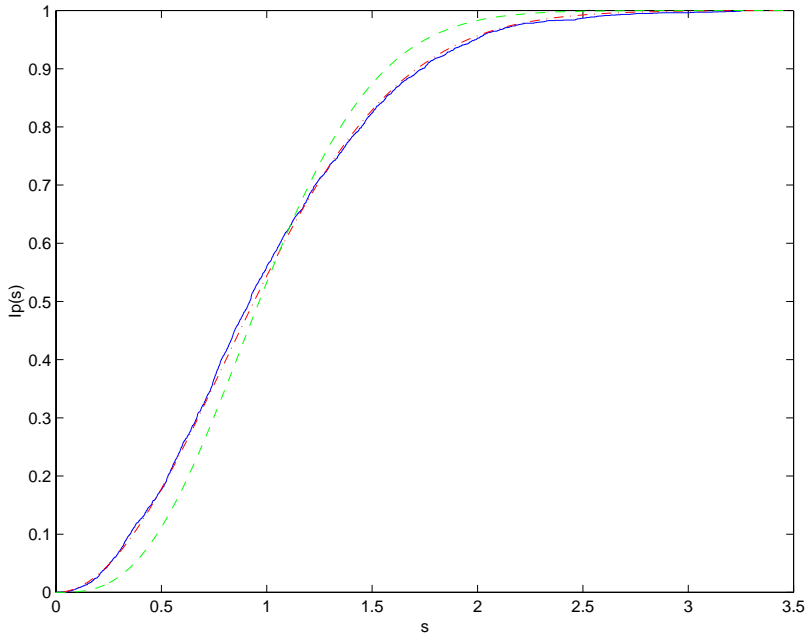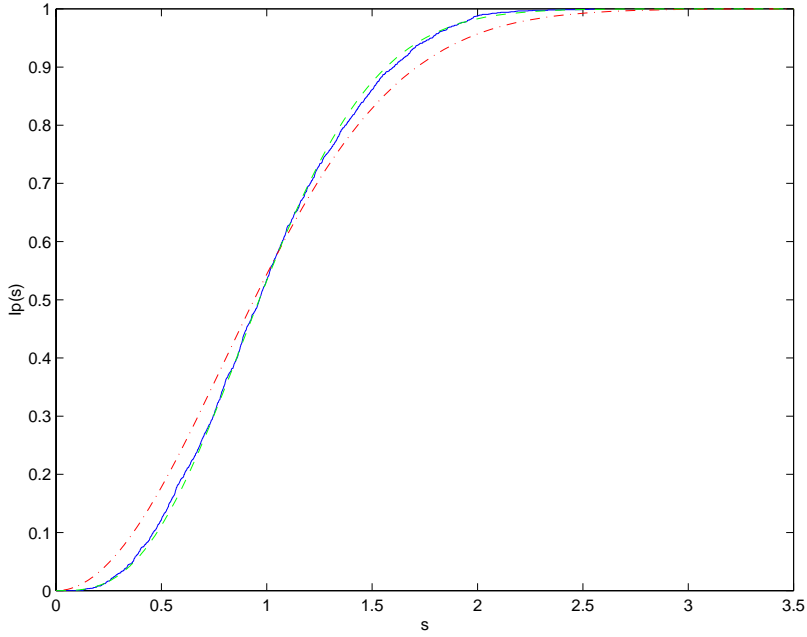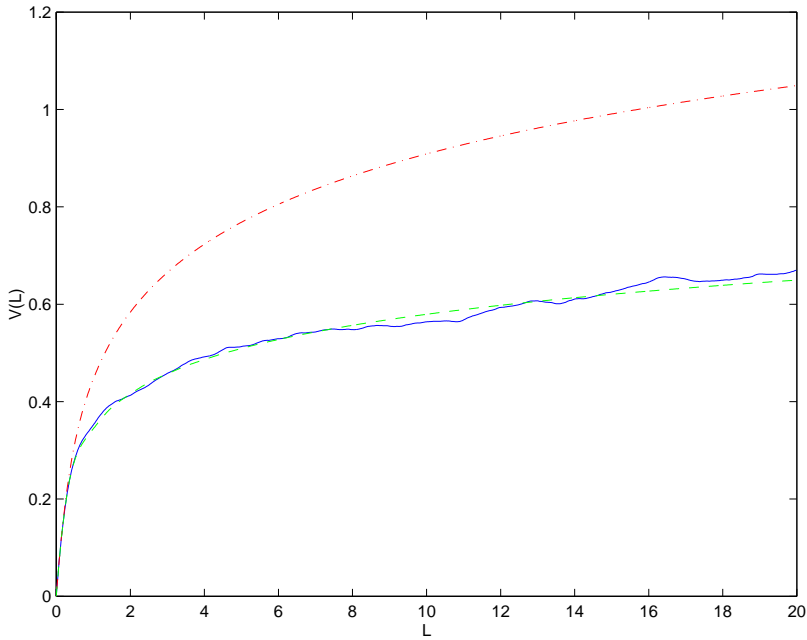
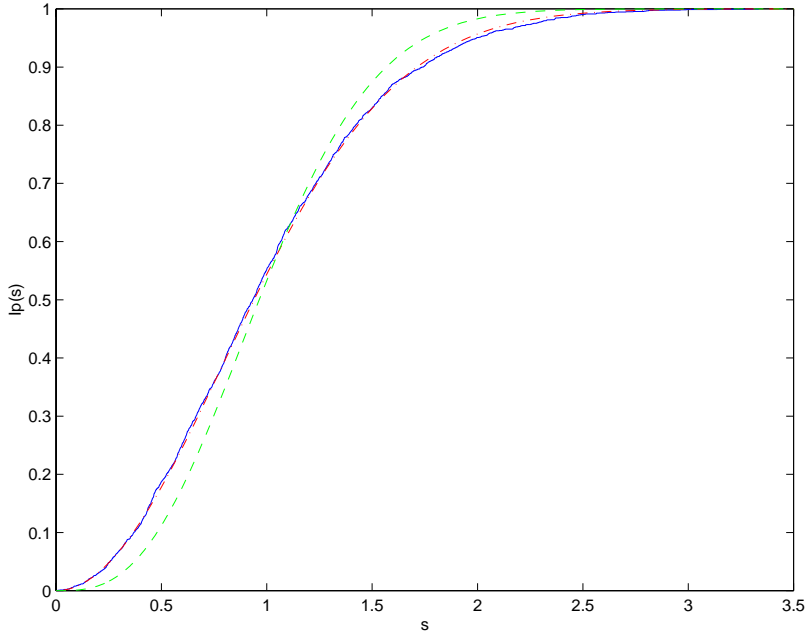(a) Cumulative spacing distribution for the map (4,9;7,16) perturbed with a shear in momentum. $N = 2447$.
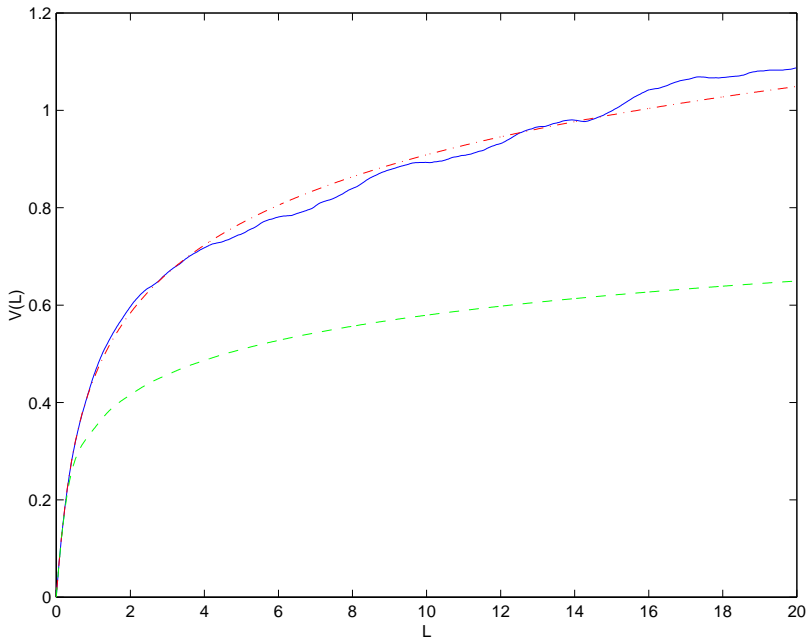
(b) Number variance for the map (4,9;7,16) perturbed with a shear in momentum. $N = 2447$.

Figure 3: The cumulative spacing distribution and number variance for the the map $(4, 9; 7, 16)$ perturbed by a shear in momentum with $k_p = 0.016$. The data, solid curves, follow the COE statistics (dot-dashed curves). The dashed curves are the CUE statistics.

(a) Cumulative spacing distribution for the map (4,9;7,16) perturbed with a composition of two shears. $N = 1993$.
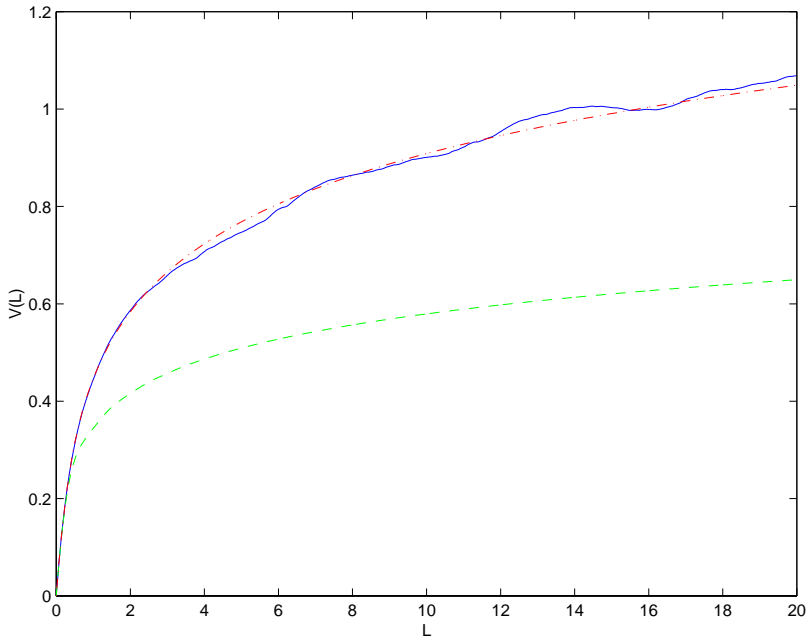

(b) Number variance for the map (4,9;7,16) perturbed with a composition two shears. $N = 1993$.

Figure 4: The cumulative spacing distribution and number variance for the map $(4, 9; 7, 16)$ perturbed by a composition of two shears with $k_p = k_q = 0.012$. The data, solid curves, follow the CUE statistics (dashed curves). The dot-dashed curves are the COE statistics.
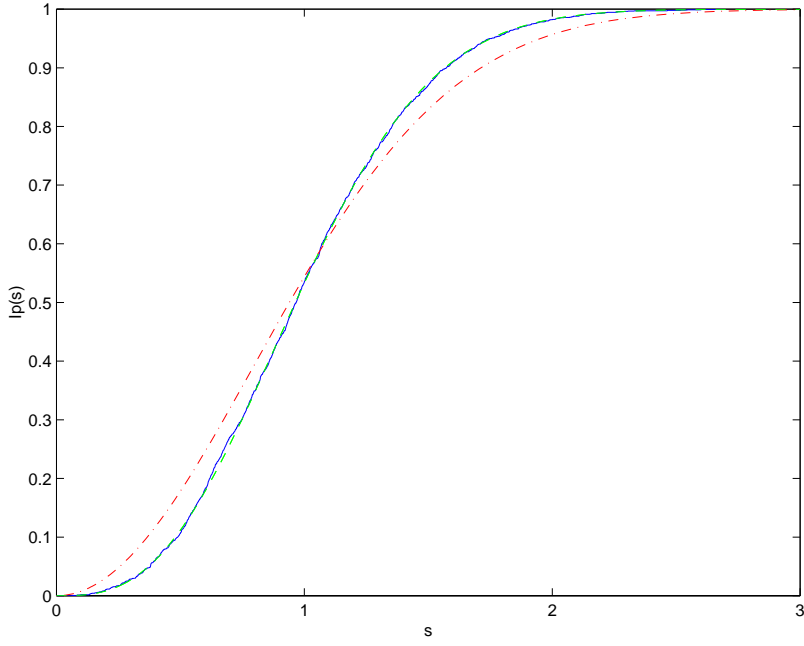
(a) Cumulative spacing distribution for the map (10,3;33,10) perturbed with a shear in momentum. $\boldsymbol{\theta} = (1/6, 5/6)$ and $N = 2417$.
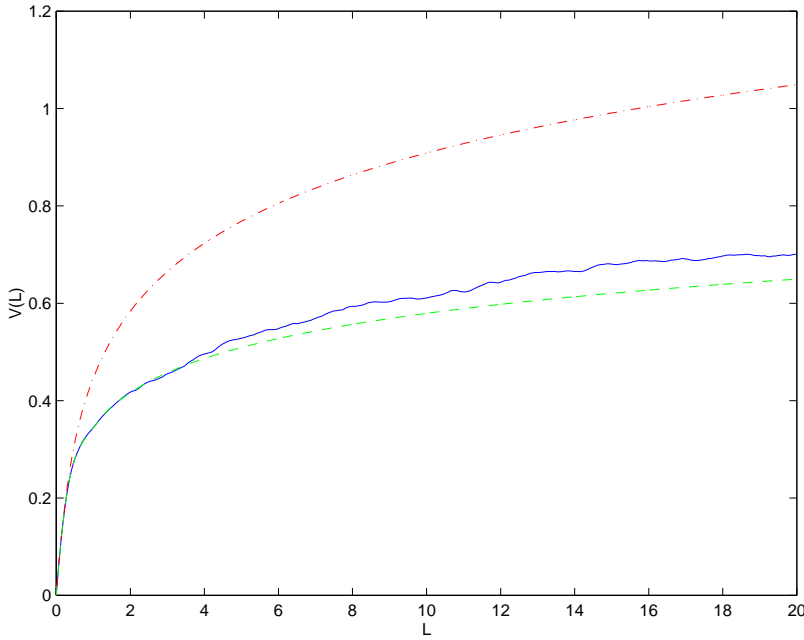

(b) Number variance for the map (10,3;33,10) perturbed with a shear in momentum. $\boldsymbol{\theta} = (1/6, 5/6)$ and $N = 2417$.

Figure 5: The cumulative spacing distribution and number variance for the map $(10, 3; 33, 10)$ perturbed by a shear in momentum with $k_p = 0.03$ and quantized with $\boldsymbol{\theta} = (1/6, 5/6)$. The data, solid curves, follow the COE curve (dot-dashed). The dashed curves are the CUE statistics.

(a) Cumulative spacing distribution for the map (10,3;33,10) perturbed with two shears. $\boldsymbol{\theta} = (1/6, 5/6)$ and $N = 1831$.

(b) Number variance for the map (10,3;33,10) perturbed with two shears. $\boldsymbol{\theta} = (1/6, 5/6)$ and $N = 1831$.

Figure 6: The cumulative spacing distribution and number variance for the map $(10, 3; 33, 10)$ perturbed by a composition of two shears with $k_p = k_q = 0.009$ and quantized with $\boldsymbol{\theta} = (1/6, 5/6)$. The data, solid curves, follow the CUE curves (dashed). The dot-dashed curves are the COE statistics.